Light Metals 2014
Edited by: John Grandfield
TMS (The Minerals, Metals & Materials Society), 2014

ASSESSMENT OF HOT CRACKING DURING TIG WELDING OF B206 ALUMINUM ALLOY

F. D'Elia[1], A. Lombardi[1], C. Ravindran[1], D. Sediako[2], K.P. Rao[3]
[1]Centre for Near-net-shape Processing of Materials, Ryerson University; 101 Gerrard St. E.; Toronto, ON, M5B 2K3, Canada
[2]Canadian Neutron Beam Centre – Chalk River Laboratories; Chalk River, ON, K0J1J0, Canada
[3]Deparment of Metallurgical and Materials Engineering, IIT-Madras; Chennai, 600036, India

Keywords: Aluminum, Varestraint Test, Hot Cracking, Residual Stress

Abstract

In this study, the hot cracking susceptibility of B206 aluminum (Al) alloy during TIG welding was investigated using the moving torch Varestraint test method. B206 Al alloy billets were cast with and without the addition of titanium-based grain refiner. The billets were then machined to 3mm thick plates and tested. In all, two levels of titanium (i.e. 0.02 and 0.05 wt%) were used. The results suggest that addition of titanium significantly reduced the hot cracking susceptibility in B206. This was attributed to a finer and more equiaxed grain structure throughout the welding regions. In addition, residual stress measurements (carried out using neutron diffraction) showed that the cracked sample contained a lower magnitude of stress as a result of relief from cracking, while a crack-free sample was found to have relatively higher magnitude of residual stress, since the stress remained 'locked-in' to resist the formation of hot cracks.

Introduction

Aluminum-copper (Al-Cu) alloys are among the most popular Al alloys in the automotive and aerospace industries. Such alloys are attractive mainly because of their excellent strength and toughness at room and elevated temperatures. B206 is a relatively new Al-Cu alloy, seen as a potential replacement for ductile iron in automotive suspension components. In the T6-treated state, this alloy has mechanical properties approaching those of ductile iron at one-third the density [1]. Therefore, use of B206 would result in significant weight savings for future vehicles.

The B206 alloy is primarily a casting alloy. However, due to its high susceptibility to hot tearing, casting of this alloy may not always be feasible, particularly when the components are complex in geometry. Hence, joining may be a viable alternative. Further, at times, welding can be used to repair broken cast components. Therefore, an investigation on the weldability of B206 is imperative in order to increase its use in industrial applications.

Hot cracking is a common defect directly impacting the weldability of alloys. Such defects occur in welding from a combination of solidification cracking in the fusion zone and liquation cracking in the partially melted zone (PMZ). During welding, the solidifying weld pool induces tensile stresses in the surrounding semi-solid material along the fusion zone, thereby promoting the formation of cracks along this region. Stresses are also generated along the PMZ from the solidifying weld pool. Cracking is facilitated along the PMZ through a reduction of strength and ductility caused by the presence of continuous liquid films along grain boundaries. Hence, the term liquation cracking is used [2, 3]. Studies [4-7] have been carried out on hot tearing of B206 during casting. However, the susceptibility of B206 to hot cracking during welding has not yet been reported.

The Varestraint test is the most commonly used method for evaluating the hot cracking susceptibility of alloys during welding [8]. The test is comprised of a welding arc, a fastened specimen, a pneumatic load and a series of die blocks. Initially, the specimen is fastened to a die block and a weld bead is deposited on the free (unfastened) side of the plate. The welding arc then moves along the plate until it reaches a pre-determined point, where a load is then applied to the unfastened portion of the plate. The load is applied exactly when the arc is extinguished, and forces the plate to conform to the radius of the die block. As a result, the strain experienced by the plate is related to the radius of the die block by the relation shown in Equation 1.

$$\varepsilon = t/2r \quad (1)$$

Where ε is the strain, t is the thickness of the plate and r is the die block curvature radius.

In this study, the Varestraint test was used to investigate the hot cracking susceptibility of B206 aluminum alloy. The effect of grain refinement on hot cracking was also examined and residual stress measurements were carried out and correlated to hot cracking susceptibility. Further, optical microscopy was performed to characterize grain structure.

Experimental Procedure

Virgin ingots of commercial grade B206 were used for all experiments. The as-received chemical composition of the B206 alloy is shown in Table I. The B206 alloy was grain refined using Al-5Ti-1B (Tibor® master alloy), whose composition is given in Table II.

Table I. Composition of B206 Alloy (wt%)

Cu	Mn	Mg	Fe	Si	Ni	Zn	Sn	Ti	Al
4.9	0.38	0.24	0.05	0.04	0.01	0.01	0.01	0.01	Bal.

Table II. Composition of Al-5Ti-1B Master Alloy (wt%)

Al	Ti	B	Fe	V	Si	Zn
93.64	5.0	1.0	0.1	0.1	0.06	0.01

The B206 alloy was melted in an electric resistance furnace. Approximately 1.5 kg of the alloy was melted in a silicon carbide crucible for each casting experiment. For each pour, the alloy was degassed at 750 °C using 0.25 wt% of sodium fluorosilicate prior to adding the Ti-B grain refiner (in rod form) to the melt at 730 °C. After five minutes of adding the Ti-B grain refiner, the melt was mechanically stirred for one minute. Finally, the melt was skimmed and poured at 700 °C.

The alloy was poured into steel billet molds (Figure 1) that were preheated to 400 °C in an electric resistance furnace. This resulted in a cooling rate of ~ 2.5 °C/s for all conditions, which was kept constant to minimize its relative effect on grain size. The molds were coated with graphite to prevent contamination of the steel with molten Al and to enable easy removal for each casting. Upon removal, the resulting billet castings were sliced to 3 mm thickness using a vertical band saw. The sliced plates were then machined to the dimensions required for the Varestraint test (i.e., 127 mm x 25 mm).

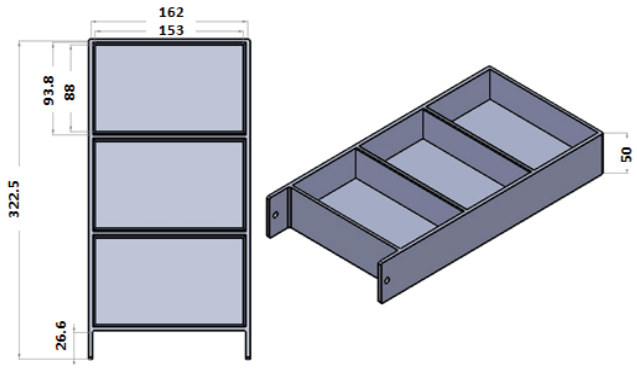

Figure 1. Steel billet molds (dimensions in mm).

The moving torch Varestraint tests were carried out at the Department of Metallurgical and Materials Engineering at IIT-Madras, in Chennai, India. The tests were performed using a strain of ε = 1.9 % (die block radius of 3.12 in.) for each condition. Tungsten inert gas (TIG) welding with argon shielding was used. A summary of the welding parameters used is presented in Table III.

Table III. Welding Parameters for Varestraint Test

Welding Parameter	Selection
Current	65 A
Heat Input	306 J/min
Weld Speed	3.5 mm/s
Voltage	15 – 18 V

Neutron diffraction strain mapping was performed at the Canadian Neutron Beam Centre in Chalk River, Canada. When a material is subjected to a tensile load, the lattice spacing of its crystal structure, d, increases in the tensile loading direction with respect to its stress-free value, d_0. The lattice spacing can be accurately measured experimentally using Bragg's law. Similarly, the lattice spacing decreases for compressive loads. Thus, the strain, ε, experienced by the material can be expressed using the peak-shift method as shown in Equation 2.

$$\varepsilon = (d - d_0)/d_0 \quad (2)$$

For an isotropic material, the relationship between stress and strain in the orthogonal Cartesian (x, y and z) coordinate system is given by the generalized form of Hooke's law (Equation 3):

$$\sigma_\alpha = E/(1+\nu)\ \{\varepsilon_\alpha + [\nu/(1-2\nu)](\varepsilon_x + \varepsilon_y + \varepsilon_z)\} \quad \alpha = (x, y, z) \quad (3)$$

Where:

ε_x, ε_y, ε_z = strain in x-, y- and z-direction, respectively
ν = Poisson's ratio
E = Young's modulus of elasticity

The experiments were carried out with a monochromatic beam of neutrons (λ = 1.55 Å), and a first-order diffraction (n = 1) analysis was performed. The (hkl) plane of interest was the (311) plane. A reference stress-free sample was obtained from the Varestraint sample. By machining the stress-free sample to 3 x 3 x 10 mm size, the remaining residual strains were relieved.

Residual stress measurements were performed on two Varestraint-tested samples: one sample with 0.02 wt% Ti addition (with hot crack) and one sample with 0.05 wt% Ti addition (without hot crack). Neutron diffraction was not carried out on the unrefined B206 condition, as the grains were too large to obtain any statistically significant measurements. The location of the linescans where measurements were obtained is indicated in Figure 2. In all, three linescans were carried out: one along the base metal, one along the heat affected zone (HAZ) and one along the weld. The location of the weld bead was at ~ x=45 mm. This location was also the point at which the welding torch paused as the die block was rammed into the specimen. Thus, it was the location where maximum strain was applied and in turn, where cracks were expected to occur.

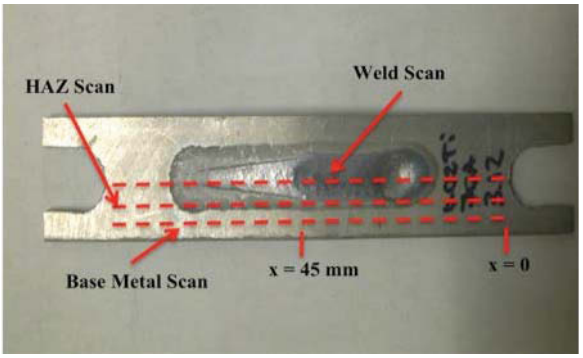

Figure 2. Linescans along the Varestraint sample.

Upon completion of the neutron diffraction experiments, the samples were sectioned and polished according to standard metallographic procedures. The polished samples were then etched to reveal grain structure using Keller's etchant and viewed under an optical microscope.

Results and Discussion

The Varestraint-tested surfaces of the B206 alloy were examined for hot cracks. Figure 3 shows the surfaces of the three tested samples. In the case of the unrefined alloy (Figure 3 a), a series of small cracks were visible on the welding surface. These cracks were seen to propagate beyond the weld and into the base metal. In contrast, the cracking on the surface of the 0.02 wt% Ti condition was less severe, as the cracks were significantly shorter and did not extend into the base metal. Lastly, 0.05 wt% Ti was found to be the optimum level of Ti for preventing hot cracking, as no cracks were found on the weld surface (Figure 3 c). Further additions of Ti were not examined as previous studies by D'Elia *et al.* [4] confirmed that Ti concentrations above 0.05 wt.% did not result in any further grain refinement.

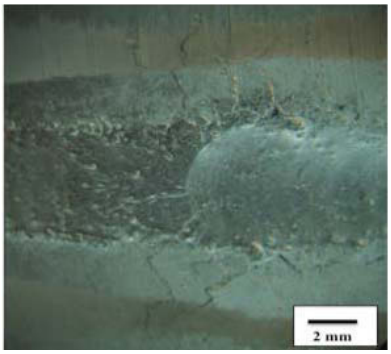

(a) Unrefined

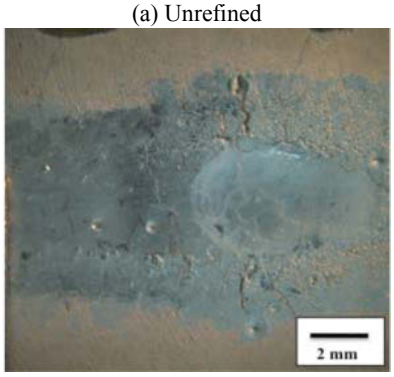

(b) 0.02 wt% Ti

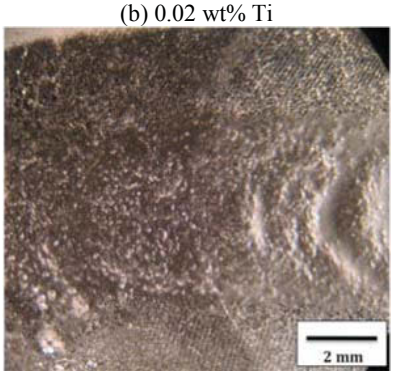

(c) 0.05 wt% Ti

Figure 3. Welding surfaces of the B206 alloy with various levels of Ti.

The grain structure of the B206 alloy is shown in Figure 4 for all the three conditions. The micrograph in Figure 4 a clearly depicts the three welding regions (i.e., fusion zone, HAZ and base metal) of the unrefined condition. These regions are labeled in the figure as FS, HAZ and BM, respectively. The base metal was characterized by a coarse dendritic microstructure, while the HAZ and fusion zone consisted of finer dendrites. This refinement in the HAZ and fusion zone was likely attributed to the high solidification rates that occurred in these regions. The dendritic structure along the three welding regions is in agreement with the hot cracks observed along these regions in Figure 3 a. The dendrites under applied loading tend to impinge on one another and therefore were likely unable to accommodate the applied strain from the Varestraint test, thereby resulting in the formation of hot cracks. Further, coarse dendrite arms are known to entrap liquid between solid grains [5], which in turn leads to embrittlement along these regions and subsequent liquation cracking. Evidence of such cracking is depicted by the arrows in Figure 4 a.

The grain structure of the 0.02 wt% Ti condition is shown in Figure 4 b. In this case, it was not possible to view the HAZ, as only the fusion zone and base metal were visible in the micrograph. The base metal for this condition appeared significantly refined in comparison to that of the unrefined condition. This region consisted of a spongy microstructure, as the grains appeared to be in transition from dendritic to globular. In turn, the globular grains were likely more resistant to the applied strain during the Varestraint test, and therefore less prone to hot crack formation. In the case of the fusion zone, however, the grain structure remained dendritic. This may have been attributed to the remelting that occurred during solidification in this region. As such, this region, unlike the base metal, was no longer able to accommodate the applied strain, and readily fractured (Figure 3 b).

The grain structure of the 0.05 wt % Ti is shown in Figure 4 c. As was the case with the 0.02 wt% Ti condition, the HAZ was not clearly visible for this condition as well. A fine equiaxed grain structure was observed along the base metal. Further, in contrast to the 0.02 wt% Ti condition, the 0.05 wt% Ti level was sufficient to enable the fusion zone to remain equiaxed as well. This was significant as it enabled the alloy resist hot crack formation during the Varestraint test. It is well established that a fine equiaxed grain structure has a greater ability to accommodate deformation, as the grains are able to slide relative to one another under loading [9]. Further, with a grain refined structure the permeability of liquid metal is improved since, relative to coarse dendrites, the grains are less branched, and therefore liquid metal can readily flow through intergranular regions and 'heal' any developing cracks.

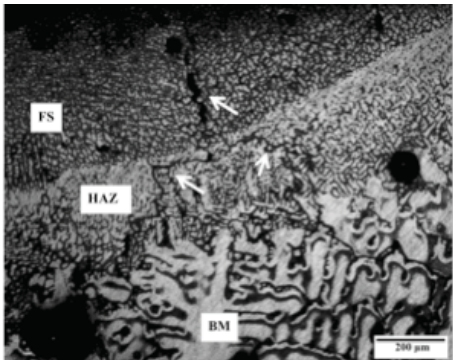

(a) Unrefined

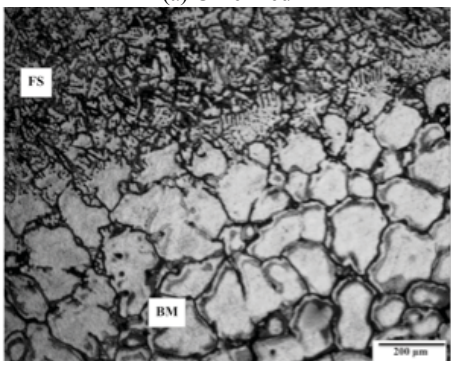

(b) 0.02 wt% Ti

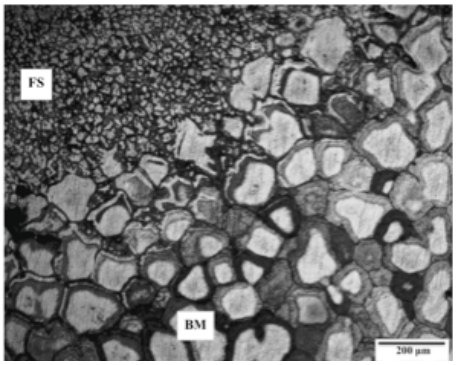

(c) 0.05 wt% Ti alloy

Figure 4. Grain structure of B206 alloy with various levels of Ti.

The plots of residual stress are shown in Figures 5 and 6 for the 0.02 wt% Ti (cracked sample) and 0.05 wt% Ti (crack-free sample) conditions, respectively. For each plot, the residual stress measurements along the base metal, HAZ and fusion zone are presented. The location of the weld bead is shaded on the graphs for each condition.

The plot of residual stress for the cracked sample depicts that the fusion zone was mainly in tension while the base metal remained in compression. The measured residual stress along the HAZ was a mix of tensile and compressive stress. The tension across the fusion zone was likely the result of the restricted shrinkage that occurred along this region. The fact that the sample was fastened during the Varestraint test did not enable the solidifying weld pool to contract freely, thereby resulting in tensile stress. Peak tension of ~ 60 MPa was observed at ~ x = 35 mm (just outside the weld bead) for the fusion zone. As the weld bead was approached, however, the stress reduced until a complete relief occurred at ~ x = 50 mm. This relief was also seen in the HAZ and was likely caused by the hot cracks that formed in the weld (Figure 3 b). In the case of the base metal, however, no crack formed in this region and therefore, no stress relief was visible. This compressive stress increased in magnitude at the location of the weld bead and as a result, was likely a reaction to the crack formation in the fusion zone and HAZ.

The residual stress profile along the crack-free sample was found to be significantly diverse from that of the cracked sample. This is illustrated in Figure 6. In the case of the cracked sample, no definite trend was observed as a mix of tensile and compressive stress was measured along the three scanned regions. This was likely the result of the solidification path of the weld. During welding, the molten weld pool is immediately surrounded by semi-solid material. The semi-solid material trailing the weld pool lies in the fusion zone, while the semi-solid material beside the weld pool lies in the HAZ (or PMZ). As the welding arc travels along the sample, solidification (i.e. contraction) is continuously taking place in the trailing semi-solid material. As such, there is a continuous 'tug of war' occurring along the fusion zone due to the differences in fraction solid with respect to the welding pool. A similar occurrence takes place in the HAZ. This 'tug of war' can explain the occurrence of the up-and-down trend observed in Figure 6. For every 'pull' there was a countering 'push', thereby maintaining the sample in equilibrium. In contrast, this did not occur in the cracked sample, as the hot cracks triggered significant stress relief, as was illustrated in Figure 5.

The overall magnitude of stress was also found to be higher in the crack-free sample relative to the cracked sample. The stress-relief caused by crack formation in the cracked sample lowered the stress magnitude. In the crack-free sample, however, the residual stresses remaining 'locked' into the sample, as no stress-relief resulted from cracking.

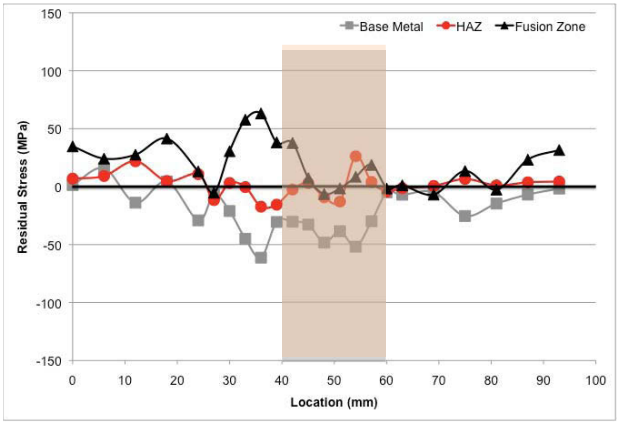

Figure 5. Residual stress profile along cracked sample.

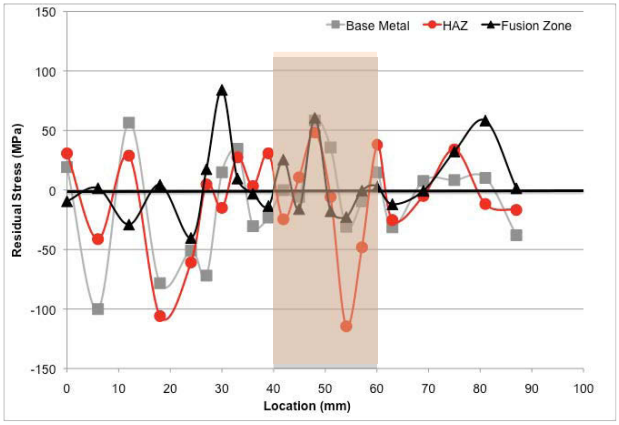

Figure 6. Residual stress profile along crack-free sample.

Conclusions

The effect of grain refinement via Ti additions was investigated on the hot cracking susceptibility of B206 Al-Cu alloy. The Varestraint test was used to carry out the analysis. The following conclusions can be drawn from this research:

1. Addition of 0.05 wt% Ti was sufficient to successfully prevent hot crack formation in B206. This level of Ti enabled the formation of a fine equiaxed grain structure along the fusion zone. In turn, these equiaxed grains were able to accommodate the strain applied during the Varestraint test, thereby resulting in no hot cracks for this condition. In contrast, the 0.02 wt% Ti level only contained an equiaxed grain structure along the base metal, which prevented hot cracks from forming in this region. The fusion zone however, was composed of a dendritic structure that was unable to resist crack formation. Lastly, the unrefined condition was fully dendritic along the fusion zone, HAZ and base metal. As a result, hot cracks formed along all regions.

2. Residual stress measurements carried out along the cracked (0.02 wt% Ti) and crack-free (0.05 wt% Ti) samples revealed diverse trends. In the case of the cracked sample, the hot cracks triggered significant stress-relief at the weld bead region, which also lowered the overall magnitude of stress in the sample. In contrast, the crack-free sample did not reveal any areas of stress-relief. As a result, the overall magnitude of stress was higher as the residual stresses remained 'locked' into the sample.
3. This study demonstrated that grain refinement can significantly improve the resistance of B206 to hot cracking. This is an important step towards characterizing and improving the weldability of B206 with a view to increasing the use of this alloy in automotive applications. Further research on the mechanical properties of B206 welds will help to further advance this study.

Acknowledgements

The authors are grateful to the Natural Sciences and Research Council of Canada (NSERC) for their financial support. They acknowledge technical assistance from the staff at the Canadian Neutron Beam Centre with neutron diffraction experiments. Further, the authors are thankful to Mr. Suriyakumar of the Department of Metallurgical and Materials Engineering at IIT-Madras for help with the Varestraint experiments, Mr. Alan Machin of Ryerson University for technical support, and the members of the Centre for Near-Net-Shape Processing of Materials (CNPM) at Ryerson University.

References

1. G.K. Sigworth and F. De Hart, "Recent Developments in the High Strength Aluminum Casting Alloys A206", *AFS Transactions*, 111 (2003), 341-354.
2. J. Lippold et al., eds., *Hot Cracking Phenomena in Welds III* (Berlin Heidelberg: Springer-Verlag, 2011), 3-23.
3. S. Kou, "Solidification and Liquation Cracking Issues in Welding", *Journal of Metals*, June 2003, 37-42.
4. F. D'Elia and C. Ravindran, "Effect of Ti-B Grain Refiner on Hot Tearing in Permanent Mold Cast B206 Aluminum Alloy", *AFS Transactions*, 117 (2009), 139-148.
5. M. Bracinni, M. Suéry and M. Stucky, "Influence of grain refinement on hot-cracking in aluminum-copper alloys", *Fonderie Fondeur d'aujourd'hui*, 208 (2001), 12-23.
6. F. D'Elia and C. Ravindran, "Influence of Grain Refinement on Hot Tearing in B206 and A319 Aluminum Alloys", *Trans. Indian Institute of Metals*, 62 (4-5) (2009), 315-319.
7. F. D'Elia, C. Ravindran and D. Sediako, "Effect of Grain Refinement on Residual Strain and Hot Tearing in B206 Aluminum Alloy" *Advanced Materials Research*, 409 (2012), 35-40.
8. C.D. Lundin, A.C. Lingenfelter, G.E. Grotke, G.G. Lessmann and S.J. Matthews, "The Varestraint Test", *Welding Research Council*, 1982, no. 280:1-19.
9. S.A. Metz and M.C. Flemings, "A Fundamental Study of Hot Tearing", *AFS Transactions*, 78 (1970), 453-460.